

Novel Descriptors for Geometrical 3D Face Analysis

FEDERICA MARCOLIN^{✉,1} AND ENRICO VEZZETTI¹

¹Department of Management and Production Engineering, Politecnico di Torino, Italy
e-mails: federica.marcolin@polito.it; enrico.vezzetti@polito.it.

ABSTRACT

3D face was recently investigated for various applications, including biometrics and diagnosis. Describing facial surface, i.e. how it bends and which kinds of patches is composed by, is the aim of studies of Face Analysis, whose ultimate goal is to identify which features could be extracted from three-dimensional faces depending on the application.

In this study, we propose 105 novel geometrical descriptors for Face Analysis. They are generated by composing primary geometrical descriptors such as mean, Gaussian, principal curvatures, shape index, curvedness, and the coefficients of the fundamental forms, and by applying standard functions such as sine, cosine, and logarithm to them. The new descriptors were mapped on 217 facial depth maps and analysed in terms of descriptiveness of facial shape and exploitability for localizing landmark points. Automatic landmark extraction stands as the final aim of this analysis.

Results showed that some newly generated descriptors were sounder than the primary ones, meaning that their local behaviours in correspondence to a landmark position is thoroughly specific and can be registered with high similarity on every face of our dataset.

KEYWORDS

3D Face; Face Analysis; landmarks; geometry; Face Recognition; Face Expression Recognition.

1 INTRODUCTION

Face Analysis has supported in these decades Face Recognition (FR), Face Expression Recognition (FER), and various medical applications such as corrective surgery, diagnosis, prenatal ultrasound. While 2D Face Analysis relies on what could be extrapolated from a facial image, such as colour or intensity [1], 3D Face Analysis represents techniques for human face study relying on three-dimensional features, such as geometrical entities like shape and curvature [2]. The third dimension was involved in the research to improve accurateness [3] and avoid issues like illumination variations [4]. 3D face data, which is often given by a non-connected point cloud, i.e. a depth map [5], allow the use of geometry and related geometrical entities in the description of facial surface. The so-generated features make it possible to compare faces and generally extract information relevant to the context of application.

Differential geometry seems to be promising for the study of facial shape and curvature behaviours, especially for applications in Face Recognition. The previous work of our research group, such as [6] [7] [8] [9] [10] [11] [12] [13] [14] [15] [16], and other contributions within the field of 3D Face Analysis, such as [17] [18] [19] [20]

[21], provided different application frameworks of entities coming from Differential Geometry context for analysing facial surfaces.

The descriptors investigated by our group have been applied to different contexts, such as recognition and medical diagnosis, and have been proven to be key 3D features for human faces at different ages. These descriptors, defined and fully explained in section 2 PRIMARY DESCRIPTORS, are: the six coefficients of the fundamental form, mean and Gaussian curvatures, principal curvatures, and shape and curvedness indexes. Some of them have been employed and mentioned in recent literature as well-performing facial features. Mean, Gaussian, principal curvatures, shape index, and curvedness, evaluated with varying neighbourhood size and bin size, were adopted as descriptors by Creusot *et al.* to support keypoints detection on 3D faces. LDA was employed to define weights to combine matching score maps over a population of neighbouring and non-neighbouring vertices, relative to the relevant landmark, and experiments were carried out on FRGC v2 [22] and BFM database [23]. Histograms of shape index (HoS) with 8 bins, the shape index itself, and principal curvatures were used to develop a mesh-based method for 3D facial expression recognition to be tested on BU3D-FE [24] [25] [26] and Bosphorus [27] databases. Mean curvature, Gaussian-weighted curvature, and spin image correlation were adopted as features by Li *et al.* [28] to detect 3D faces via graph models on IAIR-3DFace and BU3D-FE databases. Shape index, calculated for each vertex on its 5x5 neighbourhood, was used by Zhang *et al.* [29] for a face recognition method based on the adoption of six different scale invariant similarity measures. The testing was performed on FRGC v2.0. An *HK* curvature-based approach was adopted by Bagchi *et al.* [30], who developed a method for three-dimensional face detection to be applied on the FRAV3D database. *HK* indicates both mean and Gaussian curvatures. Mean and Gaussian curvature, shape index and curvedness were involved as features by Szeptycki *et al.* [31] for automatic nose tip localization on 3D faces with SVM classifier. The tested database was FRGC v2. Lanz *et al.* used mean and Gaussian curvatures for landmark detection in the context of therapeutic facial exercise recognition for patients suffering from dysfunction of facial movements [32]. The Kinect was employed for acquiring 3D faces. The same descriptors were adopted by Rabiou *et al.* for a 3D face *HK* segmentation method to be tested on UPM-3DFE and Gavab databases [33]. Zeng *et al.* involved mean curvature in a framework for facial expression recognition via conformal maps in sparse representation [34]. Tests were performed on BU-3DFER database. Abbas *et al.* tested geometrical features such as mean, Gaussian, and principal curvatures in terms of descriptiveness of facial philtrum on the three-dimensional ALSPAC database [35]. The purpose of this study was to investigate dysmorphisms around this facial area. The shape index was embedded in a facial landmark localization algorithm tested on BU-3DFE, BU-4DFE, BP4D-Spontaneous, FRGC 2.0, and Eurecom Kinect Face Dataset by Canavan *et al.* [36]. Different facial areas were classified according to mean and Gaussian curvature values in a framework of 3D surface analysis with no previous reconstruction ("one shot" technique) by Di Martino *et al.* [37]. The shape index was used as 3D local shape descriptor by Perakis *et al.* to be embedded in a feature fusion-based facial landmark detection algorithm for biometric applications [38].

Facial maps of geometrical descriptors, such as the previous 12 descriptors and the following novel ones here proposed, are alternatives to standard facial features like Gabor wavelets and Local Binary Patterns (LBPs). But, while Gabor features and LBPs have been thought and modelled for the context of image Face Analysis, i.e. working with 2D data [39], geometry-based features are strictly connected to the three-dimensional shape of surface, thus result highly suitable to the 3D context. Even if both Gabor and LBPs have been adapted to 3D data [40] [41], they are said to be lacking shape information, thus they can not carry information related to surface deformation occurring on faces in the real 3D world; this aspect significantly affects their efficient applicability to subfields for which facial deformation is a core element, such as Face Expression Recognition [39]. In particular, depth Gabor images, namely the Gabor wavelets applied to 3D data, when used alone, are said to be less descriptive of facial features than their bidimensional representatives, i.e. intensity Gabor images, as "the value of the pixels in the depth image changes less than does the value in the intensity images" [40]. In terms of inner definition, LBPs in their original meaning are histograms [42] [43], thus they are not point-by-point representations of a face; on the contrary, Gabor wavelets give two point-by-point image representations, one with the magnitude and one with the real part [44]. Nonetheless, these facial maps do not provide prompt information about facial shape. In other words, it is unrealistic to describe facial traits of a person by looking only at his/her Gabor facial image representation. Instead, this is what our primary descriptors and the novel ones try to do. Descriptors based on geometry give immediate information about position, curvature, and shape of eyes, mouth, nose, and global visage traits. These qualitative information could also be quantitatively formalized in order to give these descriptors the sound status of facial features. This is what we address in this work.

This work proposes 105 novel geometrical descriptors for 3D Face Analysis. This research partially tries to respond to the "urgent need for a robust and efficient feature representation for 3D facial shapes" [45], in particular by proposing alternative features for analysing facial surface. The idea behind the creation of these novel descriptors is rigorous in procedure, as the theoretical background of the novel descriptors lays on sound Differential Geometry principles. Also, the formulas of the newly generated descriptors rely on allowed operations for these entities, and the point-by-point properties of the original descriptors are kept. Experimentation has brought to define an hefty set of descriptors and their landmark-based specifications to be adopted for branches of Face Analysis where point-by-point facial map features, i.e. alternative facial image representations, are relevant. The final aim is also to aggregate facial information and, similarly to LBPs and Gabor jets, to create summary features which could be easily processed by the algorithms and which result to be more complete and reliable than their predecessors.

The work is structured as follows. Section 2 PRIMARY DESCRIPTORS presents the 12 geometrical primary descriptors previously used by our research group. Section 3 NEW DESCRIPTORS introduces 3.1 DERIVED DESCRIPTORS and 3.2 COMPOSED DESCRIPTORS with formulas and maps. Section 4 FEATURES highlights the features of the newly generated descriptors, with a focused analysis of their descriptiveness of landmark points. In particular, a quantification of their landmark descriptiveness is provided and discussed in section 5 DISCUSSION.

2 PRIMARY DESCRIPTORS

Classical differential geometry is the study of local properties of curves and surfaces. A patch or local surface is a differentiable mapping $x: U \rightarrow \mathbb{R}^n$, where U is an open subset of \mathbb{R}^2 . Given that a patch can be written as an n -tuple of functions

$$x(u, v) = (x_1(u, v), \dots, x_n(u, v)), \quad (1)$$

the partial derivative of x with respect to u can be defined by

$$x_u = \left(\frac{\partial x_1}{\partial u}, \dots, \frac{\partial x_n}{\partial u} \right). \quad (2)$$

The first and second fundamental forms provide the first six descriptors of the set. Their definitions rely on the possibility of measuring distances on surfaces. In Euclidean space \mathbb{R}^n , if $\underline{p} = (p_1, \dots, p_n)$ and $\underline{q} = (q_1, \dots, q_n)$ are points in \mathbb{R}^n , then the distance s from \underline{p} to \underline{q} is given by

$$s^2 = (p_1 - q_1)^2 + \dots + (p_n - q_n)^2. \quad (3)$$

Given that a general surface is curved, the distance on it is not the same as in Euclidean space; in particular, the form above is in general false however the coordinates are interpreted. To describe how to measure distance on a surface, the concept of "infinitesimal" is required. The infinitesimal version of that for $n = 2$ for a surface is

$$ds^2 = Edu^2 + 2Fdudv + Gdv^2, \quad (4)$$

called first fundamental form, or Riemann metric. This is the classical notation for a metric on a surface. E, F, G are functions $U \rightarrow \mathbb{R}$ such that:

$$E = \|x_u\|^2, \quad (5)$$

$$F = \langle x_u, x_v \rangle, \quad (6)$$

$$G = \|x_v\|^2, \quad (7)$$

and are called *coefficients of the first fundamental form*. These coefficients are given by inner products of the partial derivatives of the surface. Therefore, the first fundamental form is merely the expression of how the surface inherits the natural inner product of \mathbb{R}^3 . Geometrically, the first fundamental form allows to make measurements on the surface (lengths of curves, angles of tangent vectors, areas of regions) without referring back to the ambient space \mathbb{R}^3 where the surface lies [46].

To introduce the second fundamental form, the definitions of Gauss map must be given. For an injective patch $x: U \rightarrow \mathbb{R}^n$ the unit normal vector field or surface normal N is defined by

$$N(u, v) = \frac{x_u \times x_v}{|x_u \times x_v|}(u, v) \quad (8)$$

at those points $(u, v) \in U$ at which $x_u \times x_v$ does not vanish [47]. The map that assigns to each point p on a surface the point on the unit sphere $S^2(1) \subset \mathbb{R}^3$ that is parallel to the unit normal $N(p)$, or N_p , is called the Gauss Map.

Let $x: U \rightarrow \mathbb{R}^n$ be a regular patch. Then

$$e = -\langle N_u, x_u \rangle = \langle N, x_{uu} \rangle, \quad (9)$$

$$f = -\langle N_v, x_u \rangle = \langle N, x_{uv} \rangle = \langle N, x_{vu} \rangle = -\langle N_u, x_v \rangle, \quad (10)$$

$$g = -\langle N_v, x_v \rangle = \langle N, x_{vv} \rangle \quad (11)$$

are called the *coefficients of the second fundamental form* of x , and $edu^2 + 2fdudv + gdv^2$ is the second fundamental form of the patch x .

Very often a surface is given as the graph of a differentiable function $z = h(x, y)$, where (x, y) belong to an open set $U \rightarrow \mathbb{R}^2$. It is, therefore, convenient to be provided by formulas for the relevant concepts in this case. To obtain such formulas let us parameterize the surface by

$$x(u, v) = (u, v, h(u, v)), \quad (u, v) \in U, \quad (12)$$

where $u = x, v = y$. A simple computation shows that

$$x_u = (1, 0, h_u), \quad (13)$$

$$x_v = (0, 1, h_v), \quad (14)$$

$$x_{uu} = (0, 0, h_{uu}), \quad (15)$$

$$x_{uv} = (0, 0, h_{uv}), \quad (16)$$

$$x_{vv} = (0, 0, h_{vv}). \quad (17)$$

Thus,

$$N(x, y) = \frac{(-h_x, -h_y, 1)}{\sqrt{1+h_x^2+h_y^2}} \quad (18)$$

is a unit normal field on the surface, and the coefficients of the second fundamental form in this orientation are given by

$$e = \frac{h_{xx}}{\sqrt{1+h_x^2+h_y^2}}, \quad (19)$$

$$f = \frac{h_{xy}}{\sqrt{1+h_x^2+h_y^2}}, \quad (20)$$

$$g = \frac{h_{yy}}{\sqrt{1+h_x^2+h_y^2}}. \quad (21)$$

From the above expressions, any needed formula can be easily computed. For instance, the Coefficients of the first fundamental form are obtained [8]:

$$E = 1 + h_x^2, \quad (22)$$

$$F = h_x h_y, \quad (23)$$

$$G = 1 + h_y^2. \quad (24)$$

Beyond the six coefficients of the fundamental forms, Gaussian, mean, and principal curvatures are other four primary descriptors coming from Differential Geometry, dealt with measuring the curvature of a surface. Curvatures are used to measure how a regular surface x bends in \mathbb{R}^3 . One way to do this is to estimate how the tangent plane changes from point to point.

The two-dimensional vector subspace $Dx(q) \subset \mathbb{R}^3$, where D is the differential and q is a point of U , coincides with the set of tangent vectors to x at $x(q)$. By the above proposition, the plane $Dx(q)$, which passes through $x(q) = p$, does not depend on the parameterization. This plane will be called the tangent plane to x at p and will be denoted by $T_p(x)$. For each p there exists an orthonormal basis $\{e_1, e_2\}$ of $T_p(x)$ such that $DN_p(e_1) = -k_1 e_1$, $DN_p(e_2) = -k_2 e_2$. Moreover, k_1 and k_2 ($k_1 \geq k_2$) are the maximum and minimum of the second fundamental form restricted to the unit circle of $T_p(x)$. The maximum curvature k_1 and the minimum curvature k_2 introduced above are called the *principal curvatures* at p ; the corresponding directions, that is, the directions given by the eigenvectors e_1, e_2 are called *principal directions* at p . For instance, in the plane all directions at all points are principal directions. The same happens with a sphere. In both cases, this comes from the fact that the second fundamental form at each point is constant.

The determinant of DN is the product $(-k_1)(-k_2) = k_1 k_2$ of the principal curvatures, and the trace of DN is the negative $-(k_1 + k_2)$ of the sum of principal curvatures. If the orientation of the surface is changed, the determinant does not change (the fact that the dimension is even is essential here); the trace, however, changes sign. Particularly, in point p , the determinant of DN_p is the *Gaussian curvature* K of x at p . The negative of half of the trace of DN is called the *mean curvature* H of x at p [46]. In terms of the principal curvatures, they can be written as

$$K = k_1 k_2, \quad (25)$$

$$H = \frac{k_1 + k_2}{2}. \quad (26)$$

At an elliptic point the Gaussian curvature is positive. Both principal curvatures have the same sign, and therefore all curves passing through this point have their normal vectors pointing toward the same side of the tangent plane. The points of a sphere are elliptic points. At a hyperbolic point, the Gaussian curvature is negative. The principal curvatures have opposite signs, and therefore there are curves through p whose normal vectors at p point toward any of the sides of the tangent plane at p . At a parabolic point, the Gaussian Curvature is zero, but one of the principal curvatures is not zero. The points of a cylinder are parabolic points. Finally, at a planar point, all principal curvatures are zero. The points of a plane trivially satisfy this condition. The Gaussian curvature and the mean curvature of x are given by the formulas

$$K = \frac{eg - f^2}{EG - F^2}, \quad (27)$$

$$H = \frac{eG - 2fF + gE}{2(EG - F^2)}, \quad (28)$$

where E, F, G, e, f, g are the coefficients of the fundamental forms. Using the parameterization such that $z = h(x, y)$, an alternative form for K and H are obtained:

$$K = \frac{h_{xx}h_{yy} - h_{xy}^2}{(1 + h_x^2 + h_y^2)^2}, \quad (29)$$

$$H = \frac{(1 + h_x^2)h_{yy} - 2h_x h_y h_{xy} + (1 + h_y^2)h_{xx}}{(1 + h_x^2 + h_y^2)^{3/2}}. \quad (30)$$

The principal curvatures are the roots of the quadratic equation $x^2 - 2Hx + K = 0$. Thus, k_1 and k_2 can be chosen so that

$$k_1 = H + \sqrt{H^2 - K}, \quad (31)$$

$$k_2 = H - \sqrt{H^2 - K}. \quad (32)$$

The last two primary geometrical descriptors are the shape index and curvedness proposed by Koenderink and van Doorn [48]. The formal definition of *shape index* can be given as follows:

$$S = -\frac{2}{\pi} \arctan \frac{k_1+k_2}{k_1-k_2}, \quad S \in [-1,1], \quad k_1 \geq k_2, \quad (33)$$

It describes the shape of the surface. Koenderink and van Doorn proposed a partition of the range $[-1,1]$ in nine categories, which correspond to nine different surfaces, ranging from cup to dome/cap, but other representations exist [49] [8].

Nonetheless, the shape index does not give an indication of the scale of curvature present in the shapes. For this reason, an additional feature is introduced, the *curvedness index* of a surface:

$$C = \sqrt{\frac{k_1^2+k_2^2}{2}}. \quad (34)$$

It is a measure of how highly or gently curved a point is and is defined as the distance from the origin in the (k_1, k_2) -plane.

3 NEW DESCRIPTORS

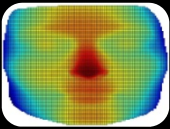
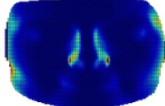
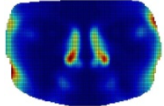
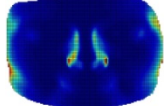
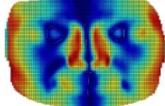
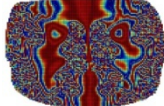
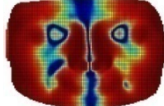
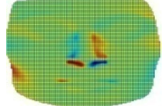
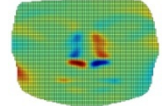
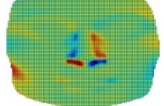
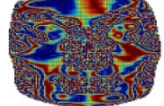
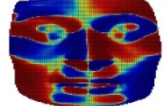
The 12 geometrical entities introduced in the previous section, which will be from now on named *primary* descriptors, have been used as theoretical basis for designing the upcoming derived and composed geometrical entities presented in the following. We have called *derived* those entities which are built from the application of a single standard function such as sine, cosine, logarithm. This classic function is directly applied to the primary descriptor to generate the derived one. *Composed* descriptors are created by combining primary descriptors. These combinations are linear combinations, fractions, products, special products of primary descriptors. They also include forms similar to those of primary descriptors.

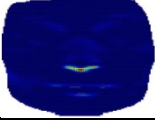
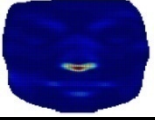
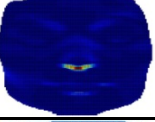
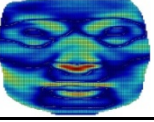
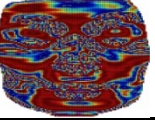
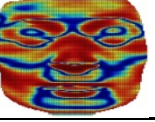
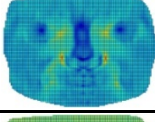
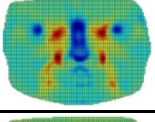
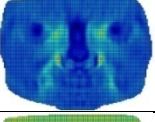
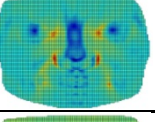
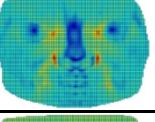
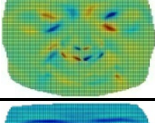
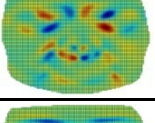
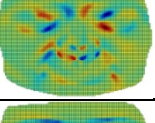
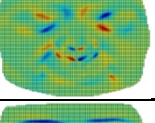
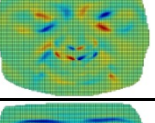
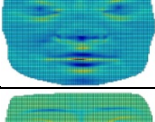
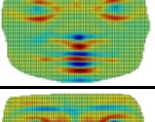
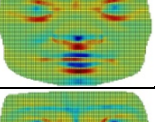
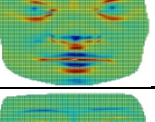
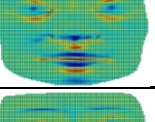
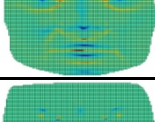
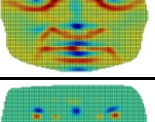
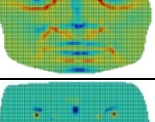
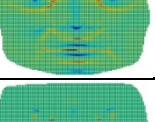
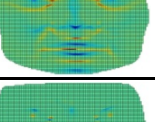
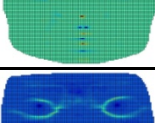
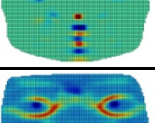
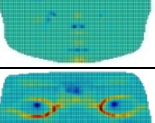
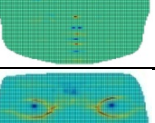
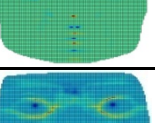
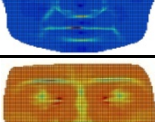
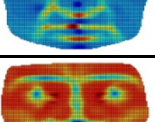
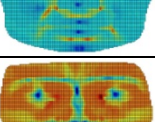
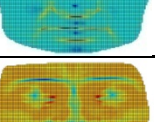
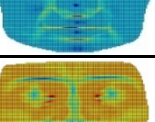
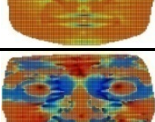
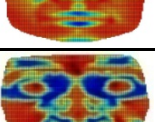
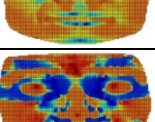
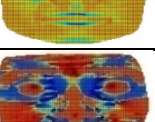
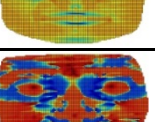
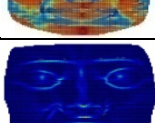
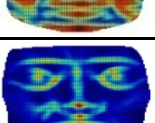
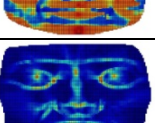
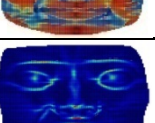
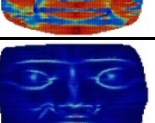

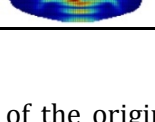
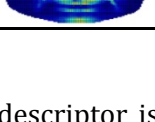
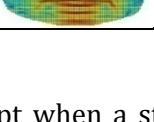


3.1 DERIVED DESCRIPTORS

Mean, median, natural logarithm, sine, cosine, tangent, arcsine, arccosine, arctangent have been applied to the 12 primary descriptors, obtaining a set of 108 derived descriptors. Mean and median were calculated in squared neighbourhoods of side 5 around each point of the facial depth maps.

The information provided by cosine was equivalent to sine in terms of quality and quantity of descriptiveness. Facial maps of arcsine gave complex values ($\in \mathbb{C}$), while tangents gave a behaviour similar to the respective original primary descriptors. For these reasons, images referred to cosines, arcsines, and tangents have not been graphically reported here, and the set of final derived descriptors taken into consideration is thus reduced to 51 items. Concerning the other derived descriptors, their "individual" point-by-point mappings onto a facial depth map are shown in Table 1. The images in this table regard only one person (female, aged 25, serious pose), whose depth map was obtained via Minolta Vivid 910 laser scanner.

Table 1. Primary (first and second columns) and derived descriptors mapped on a serious face.

		primary descriptor	mean	median	ln	sin	arctan
<i>E</i>							
<i>F</i>					$\in \mathbb{C}$		

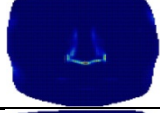
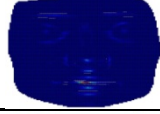




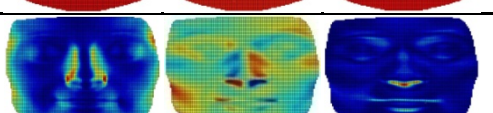
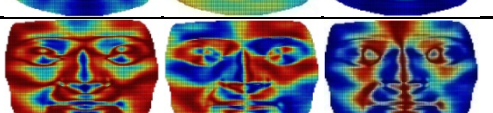
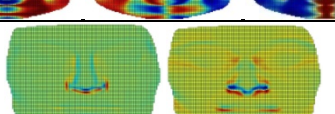
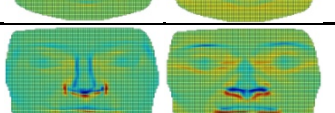
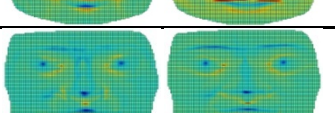
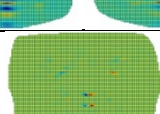


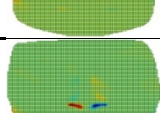
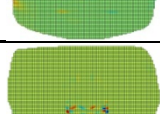
G						
e				$\in \mathbb{C}$		
f				$\in \mathbb{C}$		
g				$\in \mathbb{C}$		
H				$\in \mathbb{C}$		
K				$\in \mathbb{C}$		
k_1				$\in \mathbb{C}$		
k_2				$\in \mathbb{C}$		
S				$\in \mathbb{C}$		
C						


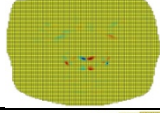
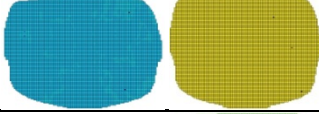
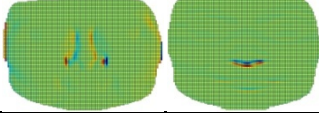
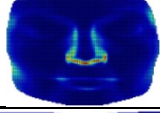
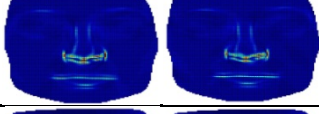
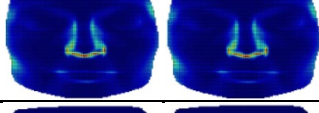
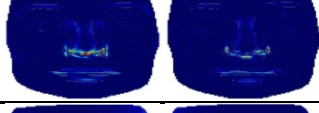
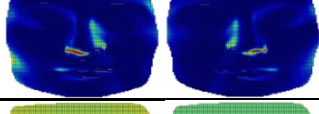
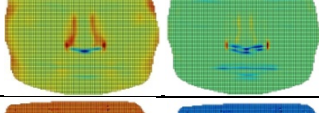
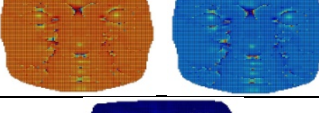
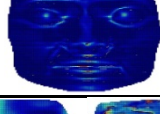
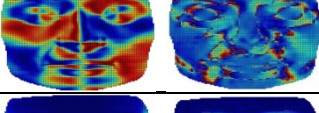
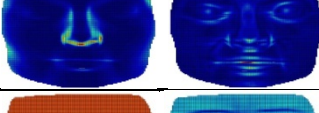
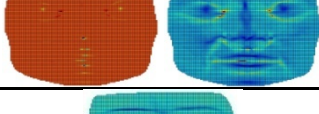
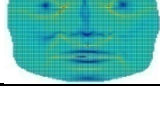
In general terms, the behaviour of the original descriptor is kept when a standard function is applied to it. Nonetheless, some of the so-generated derived descriptors better highlight local behaviours or enhance the contrast. Also, facial traits defining eyes, nose, and mouth are immediately recognizable for most of the newly-created mapped descriptors. This is a simple but crucial point in terms of descriptor usability, as a good facial descriptor allows identification of one or more facial components. Sections FEATURES and DISCUSSION will draw attention to their respective peculiarities.

3.2 COMPOSED DESCRIPTORS

Primary descriptors were also combined to generate composed descriptors, which were thought, built, and experimented by adopting standard mathematical operations such as combinations, fractions, products, special products of primary descriptors to gain novel facial representations. The new descriptors and their mappings on a face are reported in Table 2 and commented in the subsequent text. The images concern one person, the same adopted for the images of Table 1.

Table 2. Formulas (first column) and maps (second column) of composed descriptors.

Composed descriptor(s)	Map(s)
$ellipsoid_1 = E^2 + F^2 + G^2$	
$ellipsoid_2 = e^2 + f^2 + g^2$	
$ellipsoid_i = \left(\frac{e}{E}\right)^2 + \left(\frac{f}{F}\right)^2 + \left(\frac{g}{G}\right)^2$	
$ellipsoid_{ii} = \left(\frac{E}{e}\right)^2 + \left(\frac{F}{f}\right)^2 + \left(\frac{G}{g}\right)^2$	
$eE = \frac{e}{E} \quad fF = \frac{f}{F} \quad gG = \frac{g}{G}$	
$Ee = \frac{E}{e} \quad Ff = \frac{F}{f} \quad Gg = \frac{G}{g}$	
$E_{den} = \frac{E}{\sqrt{1+h_x^2+h_y^2}} \quad F_{den} = \frac{F}{\sqrt{1+h_x^2+h_y^2}} \quad G_{den} = \frac{G}{\sqrt{1+h_x^2+h_y^2}}$	
$E_{den2} = \frac{E}{1+h_x^2+h_y^2} \quad F_{den2} = \frac{F}{1+h_x^2+h_y^2} \quad G_{den2} = \frac{G}{1+h_x^2+h_y^2}$	
$EeFfGg = E \cdot e + F \cdot f + G \cdot g \quad EgFfGe = E \cdot g + F \cdot f + G \cdot e$	
$EeFfGg_{den} = \frac{E \cdot e + F \cdot f + G \cdot g}{\sqrt{1+h_x^2+h_y^2}} \quad EgFfGe_{den} = \frac{E \cdot g + F \cdot f + G \cdot e}{\sqrt{1+h_x^2+h_y^2}}$	
$EeFfGg_{den2} = \frac{E \cdot e + F \cdot f + G \cdot g}{1+h_x^2+h_y^2} \quad EgFfGe_{den2} = \frac{E \cdot g + F \cdot f + G \cdot e}{1+h_x^2+h_y^2}$	
$efg = e \cdot f \cdot g$	
$EFG = E \cdot F \cdot G$	
$EFG_{den} = \frac{E \cdot F \cdot G}{\sqrt{1+h_x^2+h_y^2}}$	
$EFG_{den2} = \frac{E \cdot F \cdot G}{1+h_x^2+h_y^2}$	
$second = h_{xx} \cdot h_{xy} \cdot h_{yy}$	

$second_{den} = \frac{h_{xx} \cdot h_{xy} \cdot h_{yy}}{\sqrt{1 + h_x^2 + h_y^2}}$	
$second_{den2} = \frac{h_{xx} \cdot h_{xy} \cdot h_{yy}}{1 + h_x^2 + h_y^2}$	
$x = \frac{h_x}{h_{xx}} \quad y = \frac{h_y}{h_{yy}}$	
$xx = h_x h_{xx} \quad yy = h_y h_{yy}$	
$cl = h_x^2 + h_y^2 + h_{xy}^2 + h_{xx}^2 + h_{yy}^2$	
$pnb_{AA+} = h_{xx}^2 + 2 \cdot h_{xy} + h_{yy}^2 \quad pnb_{AA-} = h_{xx}^2 - 2 \cdot h_{xy} + h_{yy}^2$	
$pnb_{A+} = h_x^2 + 2 \cdot h_{xy} + h_y^2 \quad pnb_{A-} = h_x^2 - 2 \cdot h_{xy} + h_y^2$	
$pnb_{BB+} = h_{xx}^2 + 2 \cdot h_{xx} \cdot h_{yy} + h_{yy}^2 \quad pnb_{BB-} = h_{xx}^2 - 2 \cdot h_{xx} \cdot h_{yy} + h_{yy}^2$	
$pnb_{B+} = h_x^2 + 2 \cdot h_x \cdot h_y + h_y^2 \quad pnb_{B-} = h_x^2 - 2 \cdot h_x \cdot h_y + h_y^2$	
$pndp_A = h_x^2 - h_y^2 \quad pndp_{AA} = h_{xx}^2 - h_{yy}^2$	
$newS_I = -\frac{2}{\pi} \arctan \frac{K+H}{K-H} \quad newS_{II} = -\frac{2}{\pi} \arctan \frac{K+H}{H-K}$	
$newC = \sqrt{\frac{K^2 + H^2}{2}}$	
$Sfond_1 = -\frac{2}{\pi} \arctan \frac{E+F+G}{E+G-F} \quad Sfond_2 = -\frac{2}{\pi} \arctan \frac{e+f+g}{e+g-f}$	
$Cfond_1 = \sqrt{\frac{E^2+F^2+G^2}{2}} \quad Cfond_2 = \sqrt{\frac{e^2+f^2+g^2}{2}}$	
$newGaussian = K \cdot H \quad newMean = \frac{K \cdot H}{2}$	
$thecurvature = \frac{k_1 + k_2 + K + H}{4}$	

The way in which the formulas of these descriptors were thought and built relies on the nature of the original formula structure of primary descriptors. Here below, the features of their concept are listed and explained.

1. The denominator in E_{den} , F_{den} , G_{den} , E_{den2} , F_{den2} , G_{den2} , $EeFfGg_{den}$, $EgFfGe_{den}$, $EeFfGg_{den2}$, $EgFfGe_{den2}$, EFG_{den} , EFG_{den2} , $second_{den}$, and $second_{den2}$ is adopted in the same form of primary descriptors (19), (20), and (21). In other words, the idea of using this denominator is taken from the formulas of e , f , and g .
2. The structure of formulas of $ellipsoid_1$, $ellipsoid_2$, $ellipsoid_i$, $ellipsoid_{ii}$, $EeFfGg$, $EgFfGe$, $EeFfGg_{den}$, $EgFfGe_{den}$, $EeFfGg_{den2}$, and $EgFfGe_{den2}$ is based on the standard equation of the ellipsoid
$$\frac{x^2}{a^2} + \frac{y^2}{b^2} + \frac{z^2}{c^2} = 1.$$
3. The concept of descriptors pnb_{AA+} , pnb_{AA-} , pnb_{A+} , pnb_{A-} , pnb_{BB+} , pnb_{BB-} , pnb_{B+} , and pnb_{B-} is based on the special product
$$(x \pm y)^2 = x^2 \pm 2xy + y^2.$$
4. The concept of descriptors $pndp_A$ and $pndp_{AA}$ is based on the special product
$$(x - y)(x + y) = x^2 - y^2.$$
5. The structure of formulas of $newS_i$, $newS_{ii}$, $Sfond_1$, and $Sfond_2$ relies on the form (33) of the shape index S . Similarly, $newC$, $Cfond_1$, and $Cfond_2$ are based on the curvedness index (34). Descriptors $newGaussian$ and $newMean$ rely respectively on Gaussian (25) and mean (26) curvatures forms.

The following section will highlight the specific features of derived and composed descriptors by drawing attention to their interesting behaviours in terms of facial descriptiveness.

4 FEATURES

The purpose of this study was to provide 3D Face Analysis research with new descriptors to be adopted as features for automatic landmarking techniques, with the possible subsequent aim to be embedded in Face Recognition and Face Expression Recognition algorithms. Also, compact forms (histograms, regional average values,...) of these novel descriptors could be directly adopted as comparison elements between faces in Face (Expression) Recognition methodologies. This section stresses the attention to the features that these new descriptors point out and is organized in subsections, each dedicated to a feature.

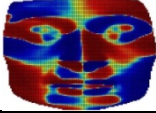
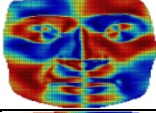
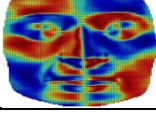
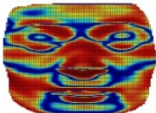
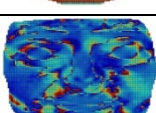
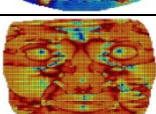
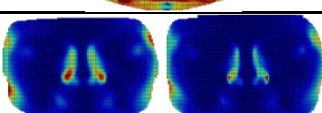
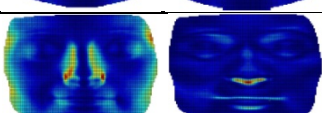
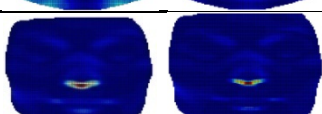
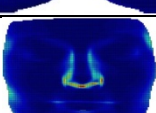
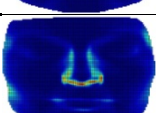
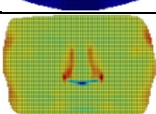
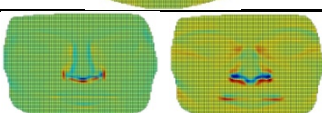
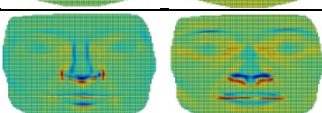
Derived and composed descriptors have been point-by-point mapped on 217 frontal-view facial depth maps of different people aged 19-32 performing 7 expressions scanned via Minolta Vivid 910 laser scanner. The scanner uses a single camera and laser stripe, and acquires 3D data using triangulation [50]. Acquisitions were single view and were made indoor in electric light conditions. The subjects were made to sit at a distance of about 1.5 meters away from the device. The laser is eye safe, so the subjects could keep their eyes open during the scanning. The scan takes approximately 2.5 seconds and the subject is asked to remain static during that time. The scanned images were then managed and useless parts such as neck and hair have been cut via reverse engineering techniques [51]. The so-generated images were then imported in Matlab® and the triangular mesh was converted into a 120x120 non-connected squared grid via function `gridtrimesh`, i.e. a depth map. The whole features analysis and subsequent graphs of Figures 6 and 7 rely on the study of the descriptors mapped on the 217 faces.

Highlighted facial lines Some new descriptors highlight facial lines. In particular, these lines are contours of facial parts such as nose, mouth, eyes, and eyebrows. Among the two sets of derived and composed descriptors, these are the ones that show visible facial parts contours: $arctan F$, F_{den2} , $Sfond_1$, $arctan G$, $Sfond_2$, $cos S$. Table 3 (above) shows them.

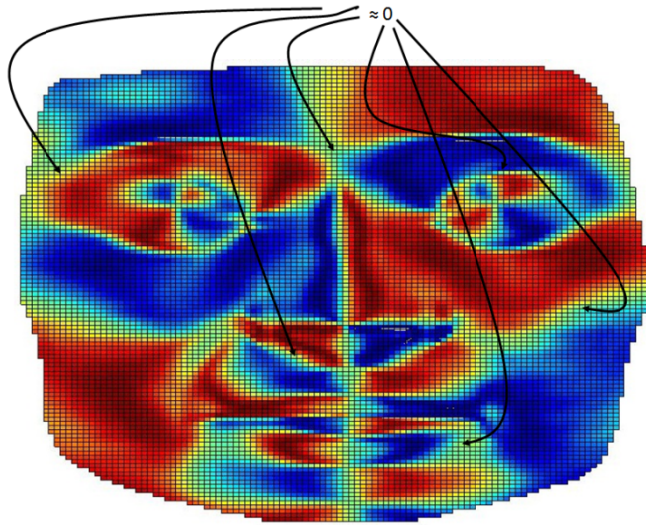
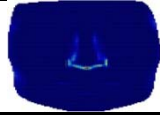
In particular, we stress the attention on those new descriptors which emphasize the **nose** shape. They are: $mean E$, $median E$, E_{den} , G_{den} , $mean G$, $median G$, $Cfond_1$, cl , $pndp_A$, $EeFfGg$, $EeFfGg_{den}$, $EgFfGe$, $EgFfGe_{den}$, $ellipsoid_1$. These descriptors are reported in the second part of Table 3. An in-depth explanation of how one of these

descriptors support the identification of facial lines is reported in Figure 1. The images concern one person, the same adopted for the images of Table 1.

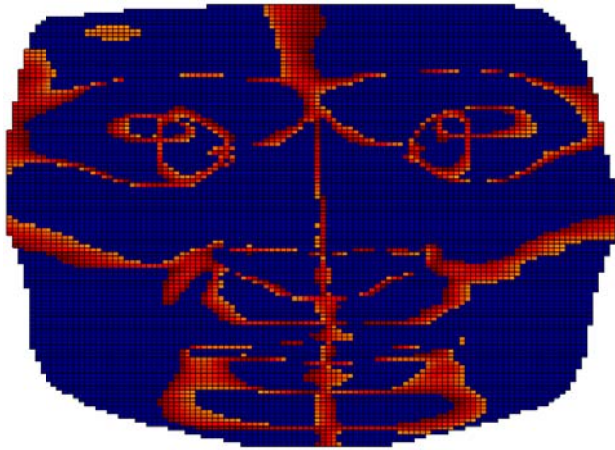
Table 3. The third column describes how the descriptor (first column) highlights facial lines. The first six rows of the table refer to descriptors with general highlighted facial lines; the other rows present descriptors which emphasize nose shape.

Descriptor	Map	Description
$arctan F$		These three descriptors allow the immediate identification of eye, eyebrow, nose, cheek, and mouth parts thanks to a clear-cut division of facial zones. The descriptor changes sign (- to + or + to -), meaning is approximately equal to zero, in correspondence to the dividing line between two zones. This behaviour is described in Figure 1.
F_{den2}		
$Sfond_1$		
$arctan G$		This descriptor assigns low (blue) values to contours and high (red) values to flat/smooth parts corresponding to specific facial zones such as nose and cheeks.
$Sfond_2$		
$cos S$		High (red) picks are associated to contours, especially in the nose and eye areas.
$mean E$ $median E$		Nose shape emphasized through high or low values of the descriptor.
E_{den} G_{den}		
$mean G$ $median G$		
$Cfond_1$		
cl		
$pndp_A$		
$EeFfGg$ $EgFfGe$		
$EeFfGg_{den}$ $EgFfGe_{den}$		

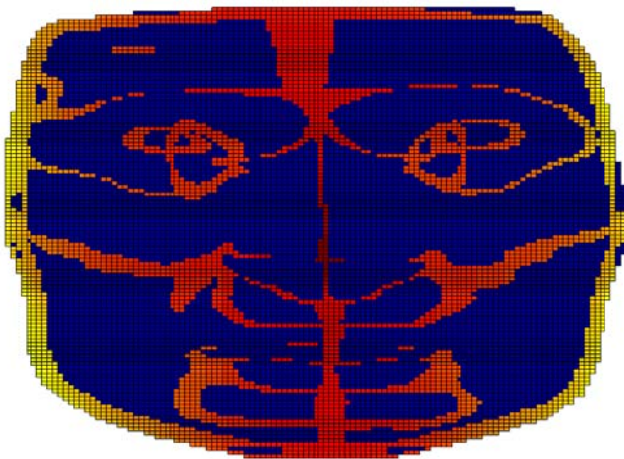
ellipsoid₁



F_{den2}



$F_{den2} \approx 0$

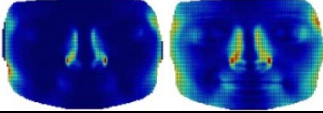
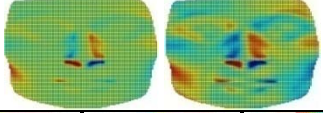
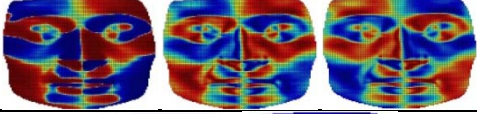
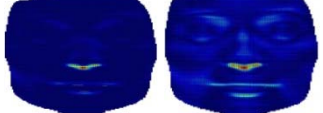

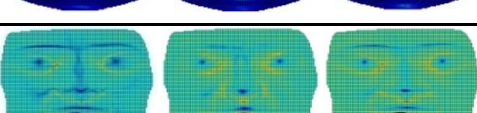


critical points ($h_x \approx 0$ and $h_y \approx 0$)

Figure 1. Above. Descriptor F_{den2} with arrows pointing to areas approximately equal to zero. Middle. Red parts show the areas of F_{den2} where the descriptor is ≈ 0 , i.e. the red points belong to a narrow neighbourhood of zero values for descriptor F_{den2} . As can be seen, the red areas form lines which correspond to dividing lines between facial zones such as nose, eyes, and mouth. Below. Reddish/yellowish points are the critical points of the original facial surface, i.e. points of the original facial depth map where derivatives with respect to x (horizontal) and y (vertical) axes are approximately equal to zero. This final image is reported to show its similarity to the middle image, as the dividing lines between facial zones conceptually correspond to critical points of the human face.

Features similar to other descriptors All derived descriptors can be associated by view to the respective original ones, with the exception of all natural logarithms, $\sin E$, $\sin F$, $\sin G$. So, it is trivial to analyze how derived descriptors are similar to their respective primary descriptors. Nonetheless, it is interesting and useful to find similarities between composed descriptors and primary, or between composed and derived ones. Table 4 and Figure 2 draw attention to these similarities. The images concern one person, the same adopted for the images of Table 1.

Table 4. Each row of the table presents a set of similar-by-view descriptors. Column 3 qualitatively contextualizes the similarity.

Descriptors	Maps	Description
E E_{den}		Highlighted lateral nose contours.
F F_{den}		An odd symmetry describes nose shape, eye zones, and mouth.
$\arctan F$ F_{den2} $Sfond_1$		An odd symmetry with strong contrast describes nose shape, eye zones, and mouth.
G G_{den}		The low part of nasal zone (subnasale point area) is highlighted.
C $Cfond_2$ $newC$		Slightly different versions of curvedness enhance facial points with higher curvature values. Their similarity is examined in Figure 2.
$the curvature$ $EeFfGg_{den2}$ $EgFfGe_{den2}$		Quality and quantity of descriptiveness similar to the curvedness but with opposite values.

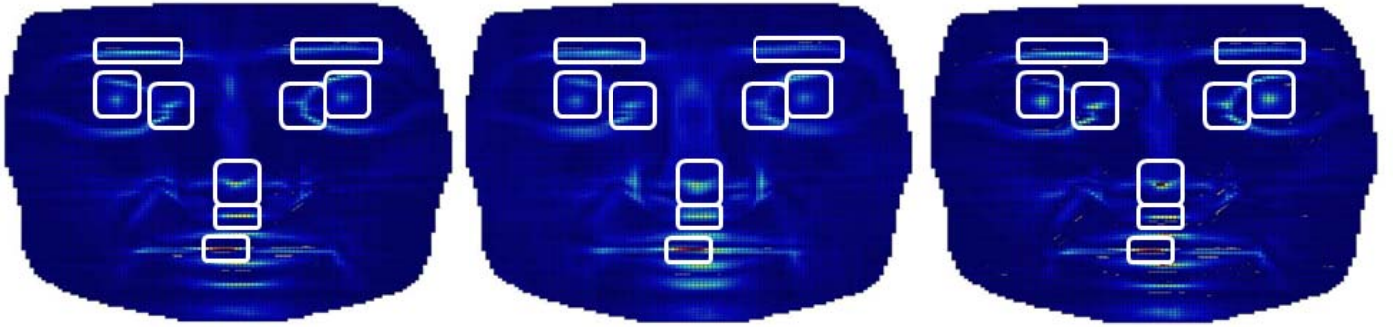


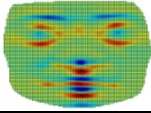
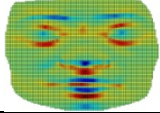
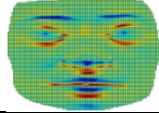
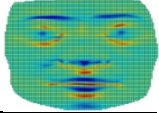
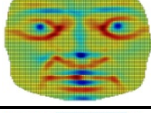
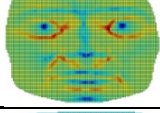
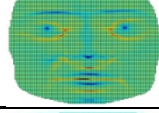
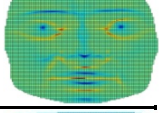
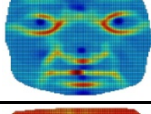
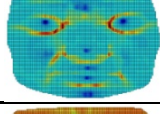
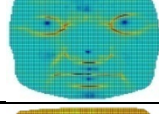
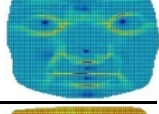
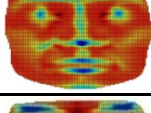
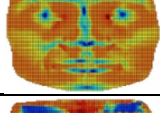
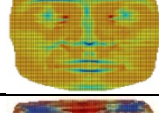
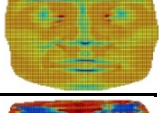
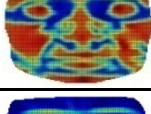
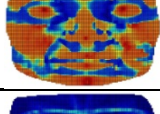
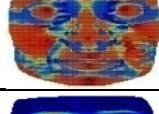
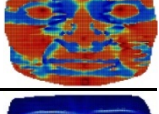
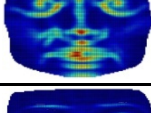
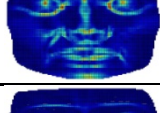
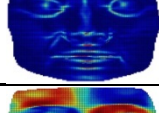

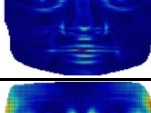
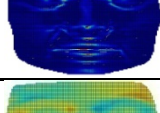
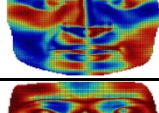
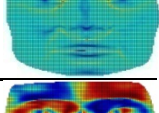
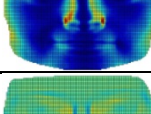
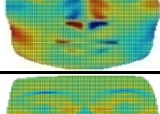
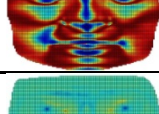
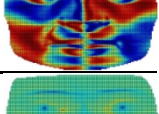
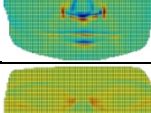
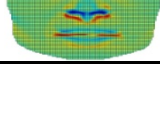
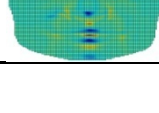
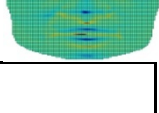
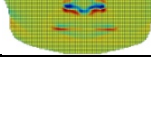
Figure 2. An example of similarity between descriptors. From left to right: C , $Cfond_2$, $newC$. The white rectangles show some local maxima in correspondence to specific points of the face such as pupils, eyebrows, nose tip (*pronasale*), *subnasale*, and the point laying on the centre of the mouth, between lips, called *stomion*. These are the most evident features that the three descriptors have in common.

These similarities could be extremely useful when a descriptor is chosen instead of another in the phase of algorithm design and construction. Although these descriptors are similar, one could better fit the issue under exam. Table 4 immediately shows similar features and differences.

Global description Many new descriptors offer a comprehensive description of the face, highlighting nose, mouth, eye areas, eyebrows in detail. Drawing attention to the 'globality' of description emphasizes the holistic nature of these new descriptors, or of at least a part of them. Differently from local features such as LBP, Gabor jets, and Scale Invariant Feature Transform (SIFT) [52], all the newly generated descriptors are holistic, or global [53]. Holistic descriptors have shown to have some advantages compared to local ones, especially in presence of different expressions, occlusions and pose variations [53].

These descriptors are reported in Table 5; one of them is studied in Figure 3. The images concern one person, the same adopted for the images of Table 1.

Table 5. List (with maps) of new descriptors presenting a global descriptive behaviour.

Descriptor	Map	Descriptor	Map	Descriptor	Map	Descriptor	Map
$mean\ g$		$median\ g$		$sin\ g$		$arctan\ g$	
$mean\ H$		$median\ H$		$sin\ H$		$arctan\ H$	
$mean\ k_1$		$median\ k_1$		$sin\ k_1$		$arctan\ k_1$	
$mean\ k_2$		$median\ k_2$		$sin\ k_2$		$arctan\ k_2$	
$mean\ S$		$median\ S$		$sin\ S$		$arctan\ S$	
$mean\ C$		$median\ C$		$sin\ C$		$arctan\ C$	
$Cfond_2$		$newC$		$Sfond_1$		$thecurvatur$ e	
E_{den}		F_{den}		E_{den2}		F_{den2}	
$EeFfGg_{den}$		$EgFfGe_{den}$		$EeFfGg_{den2}$		$EgFfGe_{den2}$	
$EgFfGe$							

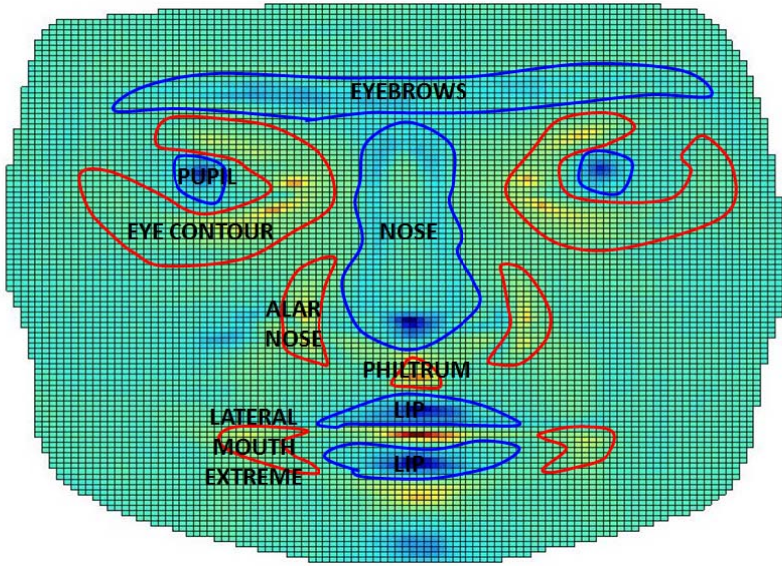


Figure 3. Descriptor $EeFfGg_{den2}$ with highlighted facial areas. The 'globality' of the description is given by the holistic behaviour of the descriptor in correspondence to every facial part; the descriptor is able to visibly identify them all. Blue lines circumscribe the facial components described by negative values of the descriptor (blue points); they are: lips, nose, eyebrows, and pupils/iris. Red lines contain the facial components represented by positive values (reddish/yellowish points); they are: lateral mouth extremes, philtrum, lateral nose parts, and eye contour. The descriptor allows a global description of the face.

The global descriptors could be core in the algorithms involving 3D Face Analysis, as the search for an alternative comprehensive map of the face is continuously carried on during research. Face Recognition and Expression Recognition techniques could benefit of new maps which highlight all facial components. In particular, compact features such as histograms, means, medians, regional or point behaviours could be extrapolated and evaluated from these global descriptors and used as comparison elements between different faces. In other words, the compact features extracted from these geometrical descriptors could constitute the core features which allow to maximize intra- or inter-person variability depending on whether the application is, respectively, Face Expression Recognition or Face Recognition. It is out of the scope of this paper to treatise how compact features could be extracted from these and other descriptors but various research contributions [7] [12] [54] exist for supporting the reader in extracting relevant information from general facial features.

Highlighted facial landmarks Many new descriptors showed local maximum or minimum behaviour on the locus of a landmark. Alternatively, some descriptors presented a typical negative or positive trend. The behaviour of each descriptor in correspondence to a landmark point has been examined on the 217 faces and then reported in Table 6; each row is dedicated to a descriptor and shows its trend among each landmark. The landmarks of Figure 4 are taken into consideration for this analysis.

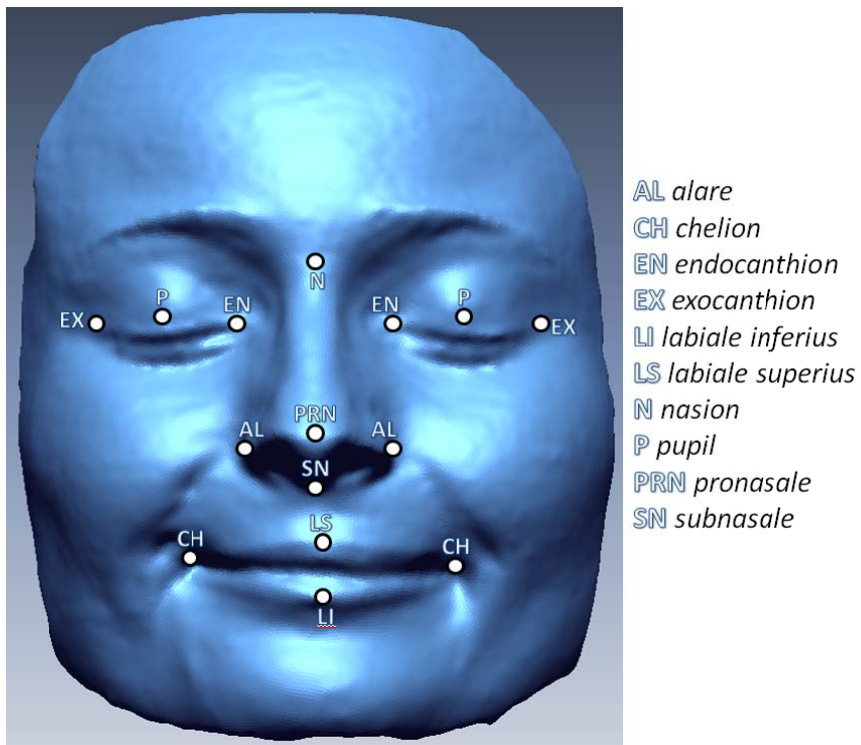
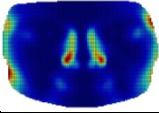
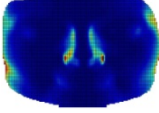
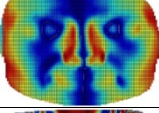
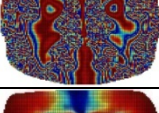
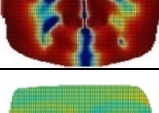
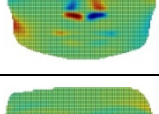
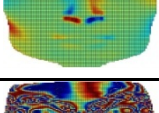
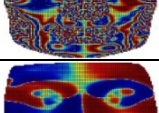
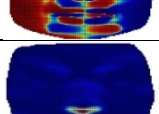
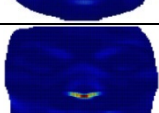
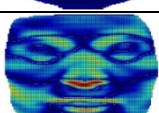
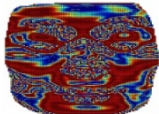
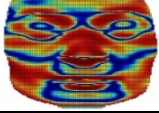

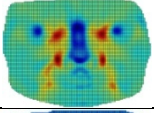
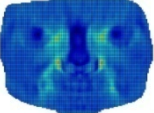
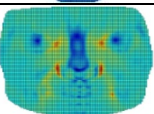
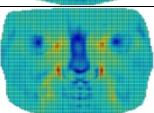
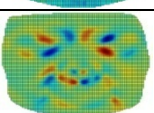
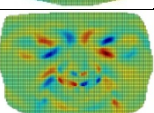
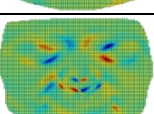
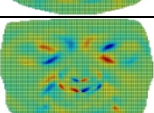
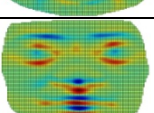
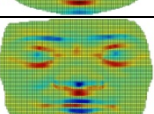
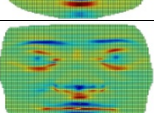
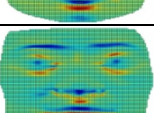
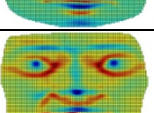
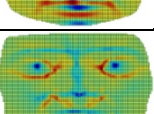
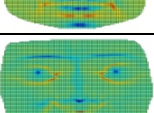
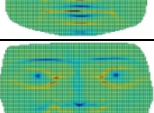
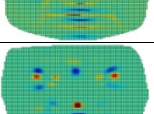
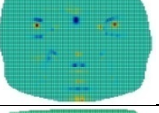
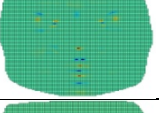
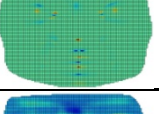
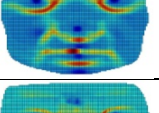
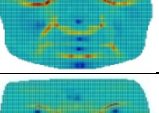
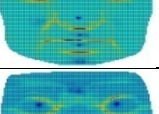
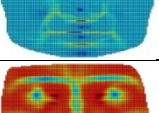
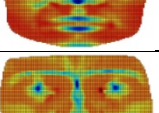
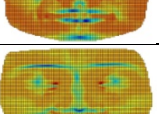
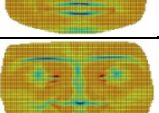
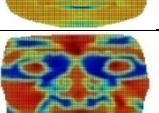
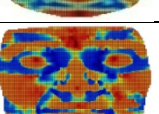
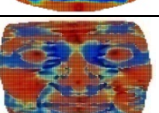
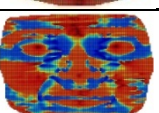
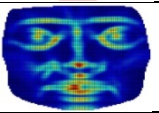
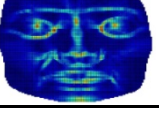



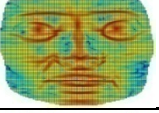


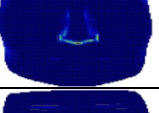
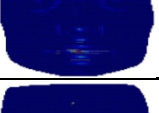
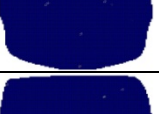
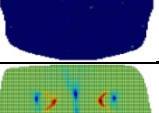
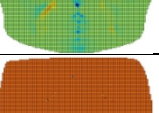
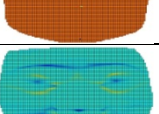
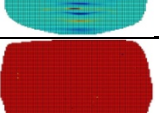

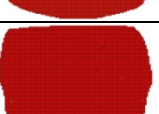
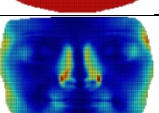
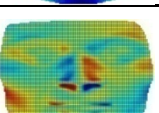


Figure 4. Soft-tissue landmarks in frontal view face adopted in this study [55].

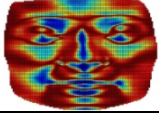
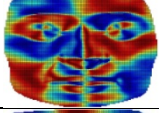
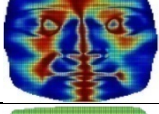
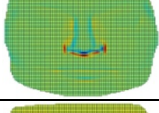
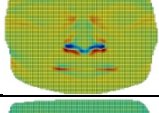
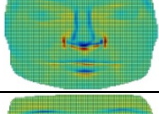
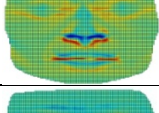
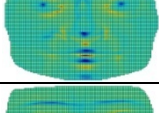
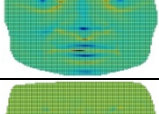
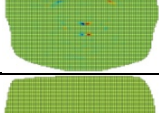
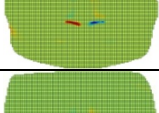
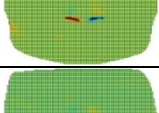


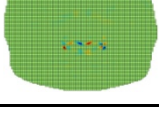
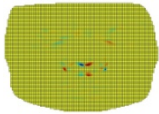
Table 6. The name of the descriptors is reported in the first column. The second column shows the related map on the same face used for Table 1. Each cell shows the behaviour of the descriptor on the locus of the landmark. **Orange** cells indicate a weak hint about the trend, meaning that slightly different behaviours are shown on different faces. **Green** cells indicate a strong hint, i.e. it is common to all faces and so it could be actually useful to extract the landmark. White boxes are neutral in terms of descriptiveness of the landmark.

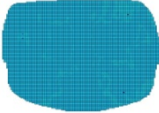
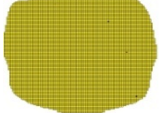
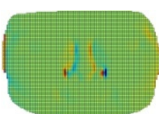
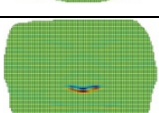
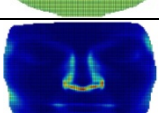
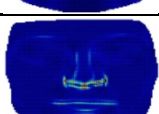
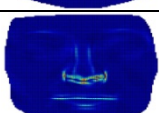
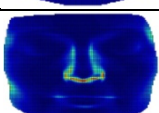
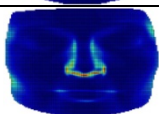
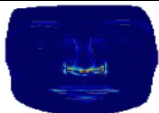
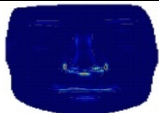
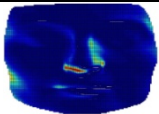
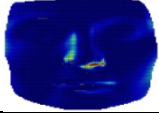
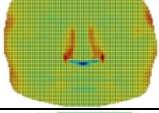
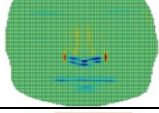
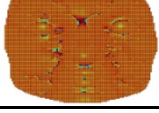
Descriptor and map		AL	CH	EN	EX	LI / LS	N	PUPILS	PRN	SN
<i>mean E</i>		MAX	MAX	<0	MAX	<0	<0	<0	<0	<0
<i>median E</i>		MAX	MAX	<0	MAX	<0	<0	<0	<0	<0
<i>ln E</i>		MAX	MAX	<0	MAX	<0	<0	MAX	<0	<0
<i>sin E</i>		nd	nd	nd	nd	>0	>0	min	>0	>0
<i>arctan E</i>		MAX	>0	<0	MAX	<0	<0	MAX	<0	<0
<i>mean F</i>		≈0	MAX sx min dx	≈0	≈0	≈0	≈0	≈0	≈0	≈0
<i>median F</i>		≈0	MAX sx min dx	≈0	≈0	≈0	≈0	≈0	≈0	≈0
<i>sin F</i>		nd	nd	nd	nd	nd	nd	nd	nd	nd
<i>arctan F</i>		>0 sx <0 dx	≈0	≈0	≈0	≈0	≈0	≈0	≈0	≈0
<i>mean G</i>		<0	<0	<0	<0	<0	<0	<0	≈0	MAX
<i>median G</i>		<0	<0	<0	<0	<0	<0	<0	≈0	MAX
<i>ln G</i>		≈0	≈0	<0	<0	>0	<0	<0	<0	MAX
<i>sin G</i>		nd	nd	nd	nd	nd	nd	nd	nd	nd
<i>arctan G</i>		>0	≈0	<0	<0	>0	<0	MAX	<0	MAX

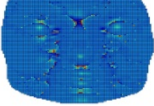

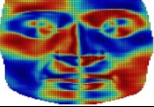
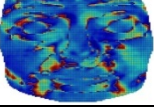
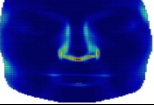

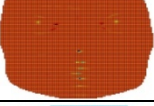
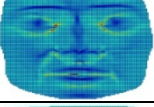
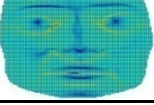
<i>mean e</i>		MAX	MAX	MAX	≈ 0	≈ 0	min	min	min	≈ 0
<i>median e</i>		MAX	MAX	MAX	MAX	< 0	min	min	< 0	≈ 0
<i>sin e</i>		MAX	MAX	MAX	MAX	≈ 0	min	min	min	≈ 0
<i>arctan e</i>		MAX	MAX	MAX	MAX	≈ 0	min	min	min	≈ 0
<i>mean f</i>		≈ 0	≈ 0	≈ 0	≈ 0	≈ 0	≈ 0	≈ 0	≈ 0	≈ 0
<i>median f</i>		≈ 0	≈ 0	≈ 0	≈ 0	≈ 0	≈ 0	≈ 0	≈ 0	≈ 0
<i>sin f</i>		≈ 0	≈ 0	≈ 0	≈ 0	≈ 0	≈ 0	≈ 0	≈ 0	≈ 0
<i>arctan f</i>		≈ 0	≈ 0	≈ 0	≈ 0	≈ 0	≈ 0	≈ 0	≈ 0	≈ 0
<i>mean g</i>		> 0	MAX	MAX	> 0	min	MAX	min	min	MAX
<i>median g</i>		> 0	MAX	MAX	> 0	min	MAX	min	min	MAX
<i>sin g</i>		> 0	MAX	MAX	> 0	min	MAX	min	min	MAX
<i>arctan g</i>		> 0	MAX	MAX	> 0	min	MAX	min	min	MAX
<i>mean H</i>		> 0	MAX	MAX	> 0	min	≈ 0	min	min	MAX
<i>median H</i>		MAX	MAX	MAX	> 0	min	min	min	min	≈ 0
<i>sin H</i>		> 0	> 0	MAX	> 0	min	≈ 0	min	min	MAX
<i>arctan H</i>		> 0	> 0	MAX	> 0	min	≈ 0	min	min	MAX
<i>mean K</i>		≈ 0	≈ 0	MAX	≈ 0	min	min	MAX	MAX	min

<i>median K</i>		≈ 0	≈ 0	≈ 0	≈ 0	min	min	MAX	MAX	min
<i>sin K</i>		≈ 0	≈ 0	≈ 0	≈ 0	min	≈ 0	MAX	MAX	min
<i>arctan K</i>		≈ 0	≈ 0	≈ 0	≈ 0	min	≈ 0	MAX	MAX	min
<i>mean k₁</i>		MAX	MAX	MAX	> 0	min	MAX	min	min	MAX
<i>median k₁</i>		MAX	MAX	MAX	> 0	min	MAX	min	min	> 0
<i>sin k₁</i>		MAX	> 0	MAX	> 0	min	≈ 0	min	min	MAX
<i>arctan k₁</i>		MAX	> 0	MAX	> 0	min	≈ 0	min	min	MAX
<i>mean k₂</i>		≈ 0	> 0	MAX	> 0	min	min	min	min	≈ 0
<i>median k₂</i>		≈ 0	> 0	MAX	> 0	min	min	min	min	≈ 0
<i>sin k₂</i>		≈ 0	MAX	MAX	> 0	min	min	min	min	≈ 0
<i>arctan k₂</i>		≈ 0	MAX	MAX	> 0	min	min	min	min	≈ 0
<i>mean S</i>		≈ 0	< 0	< 0	≈ 0	MAX	$= 0$	MAX	MAX	≈ 0
<i>median S</i>		≈ 0	< 0	< 0	≈ 0	MAX	$= 0$	MAX	MAX	≈ 0
<i>sin S</i>		≈ 0	< 0	< 0	≈ 0	MAX	$= 0$	MAX	MAX	≈ 0
<i>arctan S</i>		≈ 0	< 0	< 0	≈ 0	MAX	$= 0$	MAX	MAX	≈ 0
<i>mean C</i>		≈ 0	> 0	> 0	< 0	MAX	MAX	MAX	MAX	MAX
<i>median C</i>		≈ 0	> 0	> 0	< 0	MAX	MAX	MAX	MAX	MAX

$\ln C$		>0	>0	>0	>0	MAX	MAX	MAX	MAX	MAX
$\sin C$		≈ 0	>0	>0	<0	MAX	MAX	MAX	MAX	MAX
$\arctan C$		≈ 0	>0	>0	<0	MAX	MAX	MAX	MAX	MAX
$ellipsoid_1$		≈ 0	<0	<0	<0	<0	<0	<0	<0	<0
$ellipsoid_2$		<0	<0	<0	<0	<0	<0	<0	<0	<0
$ellipsoid_i$		<0	<0	<0	<0	<0	<0	<0	<0	<0
$ellipsoid_{ii}$		<0	<0	<0	<0	<0	<0	<0	<0	<0
eE		≈ 0	≈ 0	MAX	≈ 0	<0	min	min	min	≈ 0
fF		>0	>0	>0	>0	>0	>0	>0	>0	>0
gG		<0	≈ 0	≈ 0	≈ 0	min	≈ 0	min	min	MAX
Ee		>0	>0	>0	>0	>0	>0	>0	>0	>0
Ff		>0	>0	>0	>0	>0	>0	>0	>0	>0
Gg		>0	>0	>0	>0	>0	>0	>0	>0	>0
E_{den}		MAX	<0	<0	MAX	<0	<0	<0	<0	<0
F_{den}		≈ 0	MAX sx min dx	≈ 0	≈ 0	≈ 0	≈ 0	≈ 0	≈ 0	≈ 0
G_{den}		≈ 0	>0	<0	<0	<0	<0	<0	<0	MAX

E_{den2}		≈ 0	< 0	> 0	> 0	< 0	MAX	> 0	< 0	< 0
F_{den2}		> 0 sx < 0 dx	≈ 0	≈ 0	≈ 0	≈ 0	≈ 0	≈ 0	≈ 0	≈ 0
G_{den2}		≈ 0	> 0	< 0	< 0	> 0	> 0	min	> 0	> 0
$EeFfGg$		MAX	≈ 0	≈ 0	≈ 0	≈ 0	≈ 0	≈ 0	min	MAX
$EgFfGe$		≈ 0	MAX	MAX	> 0	≈ 0	≈ 0	≈ 0	min	≈ 0
$EeFfGg_{den}$		MAX	MAX	MAX	> 0	< 0	≈ 0	≈ 0	min	MAX
$EgFfGe_{den}$		≈ 0	MAX	MAX	> 0	< 0	≈ 0	≈ 0	≈ 0	≈ 0
$EeFfGg_{den2}$		> 0	MAX	MAX	≈ 0	min	≈ 0	≈ 0	min	MAX
$EgFfGe_{den2}$		> 0	MAX	MAX	≈ 0	min	≈ 0	≈ 0	min	MAX
efg		≈ 0	≈ 0	≈ 0	≈ 0	≈ 0	≈ 0	≈ 0	≈ 0	≈ 0
EFG		≈ 0	≈ 0	≈ 0	≈ 0	≈ 0	≈ 0	≈ 0	≈ 0	≈ 0
EFG_{den}		≈ 0	≈ 0	≈ 0	≈ 0	≈ 0	≈ 0	≈ 0	≈ 0	≈ 0
EFG_{den2}		≈ 0	≈ 0	≈ 0	≈ 0	≈ 0	≈ 0	≈ 0	≈ 0	≈ 0
$second$		MAX sx min dx	≈ 0	≈ 0	≈ 0	≈ 0	≈ 0	≈ 0	≈ 0	≈ 0
$second_{den}$		MAX sx min dx	≈ 0	≈ 0	≈ 0	≈ 0	≈ 0	≈ 0	≈ 0	≈ 0
$second_{den2}$		MAX sx min dx	≈ 0	≈ 0	≈ 0	≈ 0	≈ 0	≈ 0	≈ 0	≈ 0

x		<0	<0	<0	<0	<0	<0	<0	<0	<0
y		≈ 0	≈ 0	≈ 0	≈ 0	≈ 0	≈ 0	≈ 0	≈ 0	≈ 0
xx		MAX sx min dx	≈ 0	≈ 0	≈ 0	≈ 0	≈ 0	≈ 0	≈ 0	≈ 0
yy		≈ 0	≈ 0	≈ 0	≈ 0	≈ 0	≈ 0	≈ 0	min	MAX
cl		≈ 0	MAX	<0	<0	<0	<0	<0	<0	<0
pnb_{AA+}		MAX	>0	<0	<0	<0	<0	<0	<0	<0
pnb_{AA-}		MAX	>0	<0	<0	<0	<0	<0	<0	<0
pnb_{A+}		>0	MAX	<0	<0	<0	<0	<0	<0	<0
pnb_{A-}		>0	MAX	<0	<0	<0	<0	<0	<0	<0
pnb_{BB+}		MAX	MAX	<0	<0	<0	<0	<0	<0	<0
pnb_{BB-}		MAX	MAX	<0	<0	<0	<0	<0	<0	<0
pnb_{B+}		≈ 0	MAX sx ≈ 0 dx	<0	<0	<0	<0	<0	<0	<0
pnb_{B-}		≈ 0	≈ 0 sx MAX dx	<0	<0	<0	<0	<0	<0	<0
$pndp_A$		MAX	MAX	≈ 0	≈ 0	≈ 0	≈ 0	≈ 0	≈ 0	≈ 0
$pndp_{AA}$		MAX	min	≈ 0	≈ 0	≈ 0	≈ 0	≈ 0	≈ 0	≈ 0
$newS_I$		>0	>0	MAX	>0	>0	MAX	min	min	MAX

<i>newS_{II}</i>		<0	<0	min	<0	<0	min	MAX	MAX	min
<i>newC</i>		>0	>0	MAX	<0	MAX	<0	MAX	MAX	<0
<i>Sfond₁</i>		<0 sx >0 dx	≈0	≈0	≈0	≈0	≈0	≈0	≈0	≈0
<i>Sfond₂</i>		>0	<0	>0	>0	<0	≈0	<0	<0	<0
<i>Cfond₁</i>		MAX	MAX	<0	<0	<0	<0	<0	<0	<0
<i>Cfond₂</i>		MAX	>0	MAX	<0	MAX	<0	MAX	MAX	MAX
<i>newGaussian</i>		>0	>0	MAX	>0	min	>0	min	min	min
<i>newMean</i>		≈0	≈0	MAX	>0	min	min	min	min	min
<i>thecurvature</i>		MAX	MAX	MAX	≈0	min	<0	min	min	min

The analysis performed and presented in this table has the main aim of supporting automatic landmarking methods based on geometry [6] [7] [8] [9] [10] [11] [12] [13] [14] [15] [16].

The cells of Table 6 have been coloured relying on the reliability of the descriptor in terms of its behaviour on different faces. Figure 5 shows highlighted local behaviours of a highly consistent descriptor, *thecurvature*, on the locus of each landmark. Similar considerations could be deduced from all other descriptors. Table 7 shows the same descriptor mapped on 49 faces belonging to 7 people with 7 emotions.

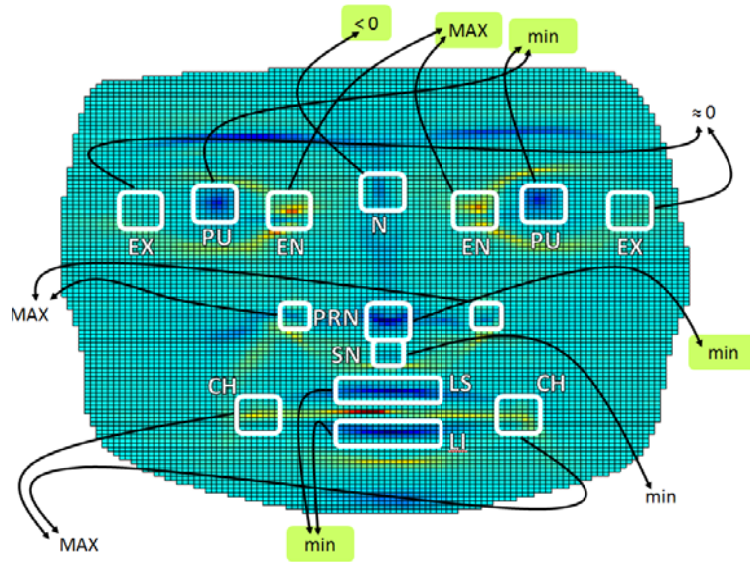


Figure 5. Descriptor *thecurvature* applied to the reference face. White squares and arrows highlight the detailed behaviour of the descriptor on the locus of each landmark, thus explaining the row referring to *thecurvature* descriptor of Table 6.

Table 7. Descriptor *thecurvature* applied to 49 faces belonging to 7 people (each row is dedicated to a person) and performing 7 expressions each (each column represents an emotion).

#	disgust	joy	fear	anger	serious	surprise	sadness
1							
2							
3							
4							
5							
6							
7							

5 DISCUSSION

The qualitative data presented in Table 6 have been quantified to determine which descriptors could be considered more suitable for landmark extraction algorithms. Value 2 has been assigned to the green boxes, representing commonality among faces and actual usability to extract the landmark; value 0 was assigned to white boxes, which are neutral in terms of descriptiveness of the landmark; value -1 was assigned to orange boxes, meaning that different behaviours are shown for these descriptors on different faces for the landmark under investigation. Thus, the criteria of evaluation is based on the soundness and reliability of the descriptor among all faces of our dataset. If a descriptor keeps the same behaviour on the locus of a landmark, the table corresponding to that descriptor and that landmark will be green and its numerical value will be assigned as 2. As said in the previous section, this quantitative study was undertaken by examining the whole set of 217 faces.

By assigning these numerical values, 'horizontal' and 'vertical' sums are calculated to state which descriptors are quantitatively more descriptive and, also, which landmarks are better described. This last landmark-based evaluation is secondary in this study, but was carried out to provide the reader with a further information about how landmarks are described with these new descriptors. Figures 6 and 7 show the global marks given by horizontal and vertical sums, respectively.

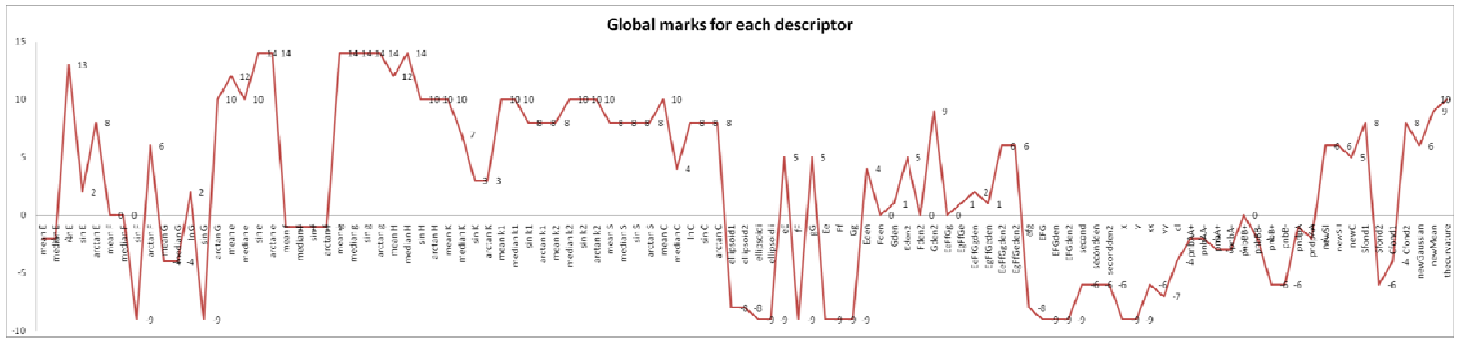


Figure 6. Global quantitative values assigned to each descriptor relying on the soundness of descriptors among different faces.

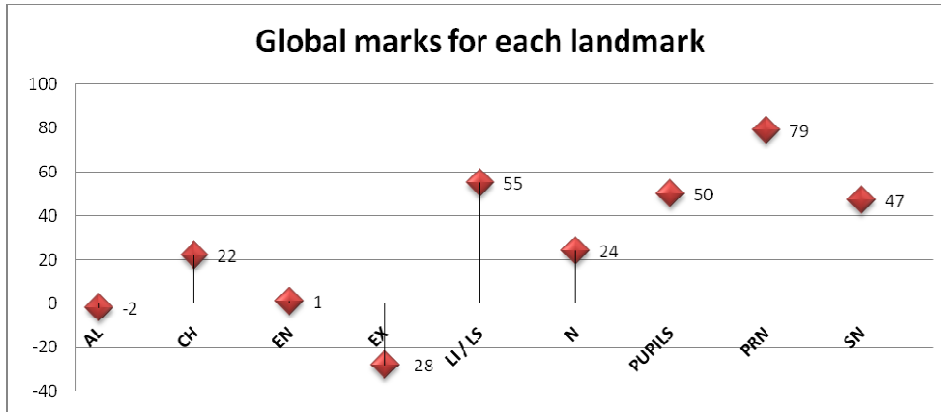


Figure 7. Global quantitative values assigned to each landmark relying on the soundness of descriptors among different faces.

The soundest and most reliable descriptors resulted *sin e*, *arctan e*, *mean g*, *median g*, *sin g*, *arctan g*, *median H*, which reached value 14, followed by *ln E*, *arctan G*, *mean e*, *median e*, *mean H*, *sin H*, *arctan H*, *mean K*, *mean k₁*, *median k₁*, *median k₂*, *sin k₂*, *arctan k₂*, *mean C*, *thecurvature*, with values in the range [10; 13]. The least reliable ones are *sin F*, *sin G*, *ellipsoid_i*, *ellipsoid_{ii}*, *fF*, *Ee*, *Ff*, *Gg*, *EFG*, *EFG_{den}*, *EFG_{den2}*, *x*, *y*, with value -9.

These results show that derived descriptors are, generally speaking, sounder than composed ones. The only composed descriptor obtaining a high mark (10) was *thecurvature*. Also, among the set of descriptors with the worst global mark, the high majority (11 up to 13) are composed descriptors.

Concerning landmarks, the landmark which reached the highest soundness in terms of descriptiveness is the pronasale (PRN) with a global mark equal to 79. It is followed by other well-described landmarks such as labial ones (mark 55), pupils (50), and subnasale (47). The worst reliability was obtained by the exocanthion, with global mark -28.

6 CONCLUSION

105 novel derived and composed geometrical descriptors for 3D face are here presented and analysed. Facial descriptiveness is taken as the core objective of descriptors' usability and innovativeness. In particular, completeness of description all over the face and particular behaviour (maximum or minimum) in correspondence to landmark points are searched for and looked as key indicators of descriptors' soundness.

The application of the new descriptors onto 217 facial depth maps acquired via laser scanner by our research group has revealed that some of them, such as those given by sine, arctangent, mean, and median of primary descriptors, are not only suitable to 3D face description and landmark localization processes, but even more accurate and clearer than their traditional predecessors. Thus, these descriptors can be considered as holistic/global features for facial surface analysis; their accessibility and legibility make them suitable for visual interpretation and appropriate for being processed by Computer Vision algorithms.

REFERENCES

- 1 Mirmehdi M, Xie X, Suri J. Handbook of texture analysis. Singapore: World Scientific Publishing; 2008.
- 2 Fanelli G, Dantone M, Gall J, Fossati A, Van Gool L. Random forests for real time 3d face analysis. *International Journal of Computer Vision*. 2013;101(3):437-458.
- 3 Kakadiaris IA. A third dimension in face recognition. DOI: 10.1117/2.1201205.004214. 2012.
- 4 Abate AF, Nappi M, Riccio D, Sabatino G. 2D and 3D face recognition: A survey. *Pattern Recognition Letters*. 2007;28(14):1885-1906.
- 5 Pears N, Heseltine T, Romero M. From 3D point clouds to pose-normalised depth maps. *International Journal of Computer Vision*. 2010;89(2-3):152-176.
- 6 Moos S, Marcolin F, Tornincasa S, Vezzetti E, Violante MG, Fracastoro G, Speranza D, Padula F. Cleft lip pathology diagnosis and foetal landmark extraction via 3D geometrical analysis. *International Journal on Interactive Design and Manufacturing*. 2014 1-18.
- 7 Vezzetti E, F. M. 3D human face description: landmarks measures and geometrical features. *Image and Vision Computing*. 2012;30(10):698-712.
- 8 Vezzetti E, F. M. Geometrical descriptors for human face morphological analysis and recognition. *Robotics and Autonomous Systems*. 2012;60(6):928-939.
- 9 Vezzetti E, F. M. Geometry-based 3D face morphology analysis: soft-tissue landmark formalization.

- 10 Vezzetti E, Marcolin F. 3D Landmarking in Multiexpression Face Analysis: A Preliminary Study on Eyebrows and Mouth. *Aesthetic Plastic Surgery*. 2014;38:796–811.
- 11 Vezzetti E, Calignano F, Moos S. Computer-aided morphological analysis for maxillo-facial diagnostic: a preliminary study. *Journal of Plastic, Reconstructive & Aesthetic Surgery*. 2010;63(2):218-226.
- 12 Vezzetti E, Marcolin F, Fracastoro G. 3D face recognition: An automatic strategy based on geometrical descriptors and landmarks. *Robotics and Autonomous Systems*. 2014;62(12):1768-1776.
- 13 Vezzetti E, Marcolin F, Stola V. 3D Human Face Soft Tissues Landmarking Method: An Advanced Approach. *Computers in Industry*. 2013;64(9):1326–1354.
- 14 Vezzetti E, Moos S, Marcolin F. Three-Dimensional Human Face Analysis: Soft Tissue Morphometry. In: *Proceedings of the InterSymp 2011*; 2011; Baden-Baden, Germany.
- 15 Vezzetti E, Moos S, Marcolin F, Stola V. A pose-independent method for 3D face landmark formalization. *Computer Methods and Programs in Biomedicine*. 2012;198(3):1078-1096.
- 16 Vezzetti E, Speranza D, Marcolin F, Fracastoro G. Exploiting 3D Ultrasound for Fetal Diagnosis Purpose through Facial Landmarking. *Image Analysis & Stereology*. 2014;33(3):167-188.
- 17 Daoudi M, Srivastava A, Veltkamp R. 3D Face Modeling, Analysis and Recognition. Chichester, West Sussex: Wiley; 2013.
- 18 Nerendra Kumar K. *Handbook of Research on Emerging Perspectives in Intelligent Pattern Recognition, Analysis, and Image Processing*. IGI; 2016.
- 19 Samir C, Srivastava A, Daoudi M, Klassen E. An intrinsic framework for analysis of facial surfaces. *International Journal of Computer Vision*. 2009;82(1):80-95.
- 20 Samir C, Srivastava A, Daoudi M. Three-dimensional face recognition using shapes of facial curves. *IEEE Transactions on Pattern Analysis and Machine Intelligence*. 2006;28(11):1858-1863.
- 21 Inan T, Halici U. 3-D face recognition with local shape descriptors. *IEEE Transactions on Information Forensics and Security*. 2012;7(2):577-587.
- 22 Creusot C, Pears N, Austin J. Automatic keypoint detection on 3D faces using a dictionary of local shapes. *International Conference on 3D Imaging, Modeling, Processing, Visualization and Transmission (3DIMPVT)*. 2011 May 204-211.
- 23 Creusot C, Pears N, Austin J. 3D landmark model discovery from a registered set of organic shapes. *IEEE ComputeSociety Conference on Computer Vision and Pattern Recognition Workshops (CVPRW)*. 2012 June 57-64.
- 24 Li H, Morvan JM, Chen L. 3d facial expression recognition based on histograms of surface differential quantities. *Advanced Concepts for Intelligent Vision Systems*. 2011 January 483-494.
- 25 Yang X, Huang D, Wang Y, Chen L. Automatic 3d facial expression recognition using geometric scattering representation. *11th IEEE International Conference and Workshops on Automatic Face and Gesture*

Recognition (FG). 2015 May;1:1-6.

- 26 Zhen Q, Huang D, Wang Y, Chen L. Muscular Movement Model Based Automatic 3D Facial Expression Recognition. *MultiMedia Modeling*. 2015 January 522-533.
- 27 Li H, Ding H, Huang D, Wang Y, Zhao X, Morvan JM, Chen L. An efficient multimodal 2D+ 3D feature-based approach to automatic facial expression recognition. *Computer Vision and Image Understanding*. 2015;140:83-92.
- 28 Li Y, Liu Y, Wang Y, Wu Z, Yang Y. 3D facial mesh detection using geometric saliency of surface. *IEEE International Conference on Multimedia and Expo (ICME)*. 2011 July 1-4.
- 29 Zhang G, Wang Y. Robust 3D face recognition based on resolution invariant features. *Pattern Recognition Letters*. 2011;32(7):1009-1019.
- 30 Bagchi P, Bhattacharjee D, Nasipuri M, Basu DK. A novel approach to nose-tip and eye corners detection using HK Curvature Analysis in case of 3D images. *Third International Conference on Emerging Applications of Information Technology (EAIT)*. 2012 November 311-315.
- 31 Szeptycki P, Ardabilian M, Chen L. Nose tip localization on 2.5 D facial models using differential geometry based point signatures and SVM classifier. *BIOSIG-Proceedings of the International Conference of the Biometrics Special Interest Group*. 2012 September 1-12.
- 32 Lanz C, Olgay BS, Denzler J, Gross HM. Automated Classification of Therapeutic Face Exercises using the Kinect. *VISAPP*. 2013 556-565.
- 33 Rabiou H, Saripan MI, Marhaban MH, Mashohor S. 3d-based face segmentation using adaptive radius. *IEEE International Conference on Signal and Image Processing Applications (ICSIPA)*. 2013 October 237-240.
- 34 Zeng W, Li H, Chen L, Morvan JM, Gu XD. An automatic 3D expression recognition framework based on sparse representation of conformal images. *10th IEEE International Conference and Workshops on Automatic Face and Gesture Recognition*. 2013 April 1-8.
- 35 Abbas H, Hicks Y, Marshall D. Automatic Classification of Facial Morphology for Medical Applications. *Procedia Computer Science*. 2015 1649-1658.
- 36 Canavan S, Liu P, Zhang X, Yin L. Landmark localization on 3D/4D range data using a shape index-based statistical shape model with global and local constraints. *Computer Vision and Image Understanding*. 2015;139:136-148.
- 37 Di Martino JM, Fernandez A, Ferrari J. 3D curvature analysis with a novel one-shot technique. *IEEE International Conference on Image Processing*. 2014 October 3818-3822.
- 38 Perakis P, Theoharis T, Kakadiaris IA. Feature fusion for facial landmark detection. *Pattern Recognition*. 2014;47(9):2783-2793.
- 39 Zhao X. 3D face analysis: landmarking, expression recognition and beyond. Lyon: Doctoral dissertation; 2011 Ecole Centrale de Lyon.
- 40 Hiremath PS, Manjunatha H. 3D Face Recognition Based on Depth and Intensity Gabor Features using Symbolic PCA and AdaBoost. *International Journal of Signal Processing, Image Processing and Pattern*

Recognition. 2013;6(5):1-12.

- 41 Tang H, Yin B, Sun Y, Hu Y. 3D face recognition using local binary patterns. *Signal Processing*. 2013;93(8):2190-2198.
- 42 Hadid A, Zhao G, Ahonen T, Pietikäinen M. Face analysis using local binary patterns. In: Mirmehdi M, Xie X, & Suri J. *Handbook of Texture Analysis*. 2008. p. 347-373.
- 43 Huang D, Shan C, Ardabilian M, Wang Y, Chen L. Local binary patterns and its application to facial image analysis: a survey. *IEEE Transactions on Systems, Man, and Cybernetics, Part C: Applications and Reviews*. 2011;41(6):765-781.
- 44 Shen L, Bai L. A review on Gabor wavelets for face recognition. *Pattern analysis and applications*. 2006;9(2-3):273-292.
- 45 Le V, Tang H, Huang TS. Expression recognition from 3D dynamic faces using robust spatio-temporal shape features. *IEEE International Conference on Automatic Face & Gesture Recognition and Workshops*. 2011 March 414-421.
- 46 Do Carmo M. *Differential Geometry of Curves and Surfaces*. Englewood Cliffs, New Jersey: Prentice-Hall Inc.; 1976.
- 47 Gray A, Abbena E, Salamon S. *Modern Differential Geometry of Curves and Surfaces with Mathematica*. Boca Raton, Florida: CRC Press; 2006.
- 48 Koenderink JJ, van Doorn AJ. Surface shape and curvature scales. *Image and vision computing*. 1992;10(8):557-564.
- 49 Dorai C, Jain AK. COSMOS-A representation scheme for 3D free-form objects. *IEEE Transactions on Pattern Analysis and Machine Intelligence*. 1997;19(10):1115-1130.
- 50 Vezzetti E. Computer aided inspection: design of customer-oriented benchmark for noncontact 3D scanner evaluation. *The International Journal of Advanced Manufacturing Technology*. 2009;41(11-12):1140-1151.
- 51 Vezzetti E. Adaptive sampling plan design methodology for reverse engineering acquisition. *The International Journal of Advanced Manufacturing Technology*. 2009;42(7-8):780-792.
- 52 Bennamoun M, Guo Y, Soheli F. Feature selection for 2D and 3D face recognition. *Wiley Encyclopedia of Electrical and Electronics Engineering*. 2015.
- 53 Meethongjan K, & Mohamad D. *A Summary of literature review: Face Recognition*. 2007.
- 54 Liu Y, Li C, Su B, Wang H. Evaluation of feature extraction methods for face recognition. *IEEE Sixth International Symposium on Computational Intelligence and Design (ISCID)*. 2013 October;2:313-316.
- 55 Swennen GR, Schutyser FA, Hausamen JE. *Three-dimensional cephalometry: a color atlas and manual*. Springer Science & Business Media; 2005.